

# Accepted Manuscript

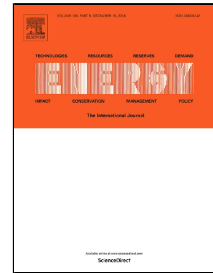
Detailed Study, Multi-Objective Optimization, and Design of an AC-DC Smart Microgrid with Hybrid Renewable Energy Resources

Mohammad Ghiasi

PII: S0360-5442(18)32449-6  
DOI: 10.1016/j.energy.2018.12.083  
Reference: EGY 14336  
To appear in: *Energy*  
Received Date: 03 October 2018  
Accepted Date: 12 December 2018

Please cite this article as: Mohammad Ghiasi, Detailed Study, Multi-Objective Optimization, and Design of an AC-DC Smart Microgrid with Hybrid Renewable Energy Resources, *Energy* (2018), doi: 10.1016/j.energy.2018.12.083

This is a PDF file of an unedited manuscript that has been accepted for publication. As a service to our customers we are providing this early version of the manuscript. The manuscript will undergo copyediting, typesetting, and review of the resulting proof before it is published in its final form. Please note that during the production process errors may be discovered which could affect the content, and all legal disclaimers that apply to the journal pertain.



# Detailed Study, Multi-Objective Optimization, and Design of an AC-DC Smart Microgrid with Hybrid Renewable Energy Resources

Mohammad Ghiasi<sup>1,2</sup>

<sup>1</sup> Power Control Center (PCC), Tehran Metro, Tehran Urban and Suburban Railway Operation Co (TUSRC), Tehran, Iran

<sup>2</sup> Metro College, University of Applied Science and Technology, Tehran, Iran  
Email: [Ghiasi1984@gmail.com](mailto:Ghiasi1984@gmail.com)

**Abstract:** Hybrid renewable system is a particular type of energy systems which can be used as Distributed Generation (DG) resources to reduce network losses and increase its efficiency. Overall, at design phase, there are two major constraints: first, availability, and second, the cost of equipment. In this paper, considering these constraints and using DGs as Renewable Energy Sources (RES) including wind turbines and photovoltaics, an intelligent method based on multi-objective particle swarm optimization is utilized. Besides, battery bank has been used as a backup unit and energy storage of the hybrid system to reduce the volatility of RESs. The purposes of this paper are: to provide a comprehensive analysis on new structures of AC and DC systems, and then, to determine the capacity and optimal design with hybrid RESs in a smart microgrid to increase the availability and reduce network costs. In order to demonstrate the possibility of proposed approach, an optimized method is designed and implemented in two scenarios (Basic, and Maximum Renewable). Effectiveness of the proposed approach is applied over a real study case. By comparing the proposed method with multi-objective genetic algorithm, simulation results show that the proposed method has effective performance in reducing costs and improving availability.

**Keywords:** AC-DC Systems; Distributed Generation; Microgrids; Renewable Energy Resources.

## Nomenclatures

$A$	Availability Index	$\alpha_{Wind}$	Cost of Wind Turbine
$A_{Photovoltaic}$	Panel Surface	$\alpha_{Battery}$	Cost of Battery Bank
$A_{Wind}$	Surface Area of Winding for Turbine	$\beta$	Inflation Rate
$C_{Wind}$	Initial Cost	$\Delta P$	Demand Not Met (kWh/Y)
$C_{Network}$	Cost of Power Input From Network	$\partial$	Ratio of Input Power From Network to Load
$C_{Battery}$	Initial Cost of Battery	$\nu$	Escalation Rate
$C_i$	Initial Cost of Each Component	$\gamma$	Interest Rate
$Cost$	Total System Cost Per Dollar Per Year	$\omega$	WTG Speed (Rad Per Sec)
$D$	Demand	<b>List of Abbreviations</b>	
$J$	Inertia (Kg.M <sup>2</sup> )	$CCT$	Clearing Critical Time
$M_iO$	Operating And Maintenance Cost of Each Component	$DG$	Distributed Generation
$N$	Lifetime of System	$ESS$	Energy Storage System
$OM_{Battery}$	Total Cost of Operation and Maintenance for Battery System	$EMA$	Energy Management Algorithm
$OM_{yearly}$	Annual Operating and Maintenance Cost	$EV$	Electric Vehicles
$OM_{Wind}$	Total Cost of Operation And	$GW$	Gigawatt

	Maintenance of Wind Subsystem		
$P_e$	Wind Turbine Electrical Power (W)	<b>HES</b>	Hybrid Energy Storage System
$P_{Battery}$	Bank Capacity of Battery	<b>HVDC</b>	High Voltage Direct Current
$P_s(t)$	Total Instantaneous Power Delivered by ESS (W)	<b>LCC</b>	Line Commutated Converter
$P_g(t)$	Total Instantaneous Power of Generating Sources (W)	<b>MOGA</b>	Multi-Objective Genetic Algorithm
$P_{Network,t}$	Power Purchased From Network	<b>MTDC</b>	Multi-Terminal Direct Current
$P_m$	Wind Turbine Mechanical Power (W)	<b>MOPSO</b>	Multi-Objective Particle Swarm Optimization
$P_{load}(t)$	Instantaneous Load Power (W)	<b>MPC</b>	Model Predictive Control
$P_{BatteryMin}(t)$	Minimum Charge of Battery Bank in Time	<b>PV</b>	Photovoltaic
$P_{BatterySOC}(t)$	Battery Charge Status in Time	<b>RES</b>	Renewable Energy Resource
$P_D(t)$	Amount of Demand in Time Unit	<b>SoC</b>	State of Charge
$U(t)$	Step Function	<b>VSC</b>	Voltage Source Converter
$\alpha_{Photovoltaic}$	Cost of Solar Panel	<b>W</b>	Watt
$\alpha_{Network}$	Cost of Input Power From Network	<b>WTG</b>	Wind Turbine Generator

## 1. Introduction

### 1.1. Background

Current trends indicate that global electricity distribution grids are experiencing a transformation towards DC at both generation and consumption level. This kind of tendency is powered by the outburst of different electronic loads and, simultaneously, with the struggle to meet the high set aims for share of RESs in satisfying total demand [1, 2]. Meanwhile, with increasing energy growth and reduction in fossil fuel resources, renewable energies such as solar and wind can play vital role in development of countries; accordingly, due to environmental problems and global warming, we need to preserve our environment, decreasing air pollution, and considering electricity constraints and energy supply for urban, remote and rural areas. On the other hand, the political and economic backing of countries depends on their productivity from fossil fuels. Reducing fossil fuel resources is not only a threat to the economies of the exporting countries, but also a major concern for other energy-consuming countries. Another issue that should be considered is the security of the power system. Maintaining a high level of system security is one of the most important aspects of power systems that should be noted as well as the economic operation of these systems [3-7].

In addition, energy consumption prediction can play an important role in design, planning and management of power systems. It can be said that an accurate forecasting of electric energy consumption provides more realistic spectrum for consumption of future country's energy resources to move towards sustainable development in globalization [8, 9]. As can be seen from the reference [10], at the beginning of the year 2016, the amount of installed Photovoltaic (PV) and wind energy in the European (EU) countries reached to capacity of approximately 95.5 Gigawatt (GW) and 141.6 GW respectively, that correspond to 10.5% and 15.6% of the total EU electricity generation capacity. In addition, the amount of Renewable Energy Sources (RES) has increased its share from 24% in 2000 to 44% of total power capacity at the beginning of 2016; also, during 2016, at least 75 GW of solar PV capacity was added globally which equivalent to the installation of approximately more than 31,000 solar panels every hour. By 2020, wind power is expected to feed nearly 10% of global electricity.

## 1.2. Literature Review

In recent decades, DC technology has entered into a new Renaissance period of time, because of several generations after Westinghouse and Edison's public battles facing AC versus DC in the famous "war of currents", back by 1880 [11]. In this regard, we provide an overview of transmission and distribution systems in AC and DC grids. The reference [12] has expressed that DC systems rebooting started in 1954, when ABB company linked the island of Gotland to the Swedish mainland by a High Voltage Direct Current (HVDC) link, delivering the world's first commercial HVDC system. According to the type of load flow and load demands, microgrid can be categorized as AC microgrid and DC microgrid. Some relative topics including harmonic current, the flow of reactive power, transformer failures, and unbalanced phases in AC microgrid open the door to promote DC microgrid with DC loads and DC supply from PV and Fuel Cells (FC) and other RES. Some professions are of the view that a normal distribution grid system consists of both AC and DC loads, which AC power cannot be totally neglected as connecting a DC resource to high AC load gains harmonic content and converter losses [13, 14].

Moreover, in this field, one of the interesting topics that recently researchers are working on is Multi-Terminal Direct Current (MTDC); hence, in the references [12, 15], some critical challenges and prospects for this kind of emerging MTDC networks, along with a foreseeable technology improvement road map, with a particular focus on decisive operational and control issues that are associated with MTDC systems and networks are presented. As explained in these references, two serious power conversion technologies have traditionally dominated by HVDC designs, titled the Voltage Source Converter (VSC), and the Line Commutated Converter (LCC); which both have been deployed and commercialized across today's global grids. Figure 1 shows a simple typical representation of an AC overlaid MTDC network containing several LCC-HVDC and VSC-HVDC terminals. Also, reference [16] presented a new approach to select an optimal place and control variable setting for Power Flow Controllers (PFC) including series, cascaded, and interline PFCs in MT-HVDC networks based on sensitivity analysis method to enhance static security.

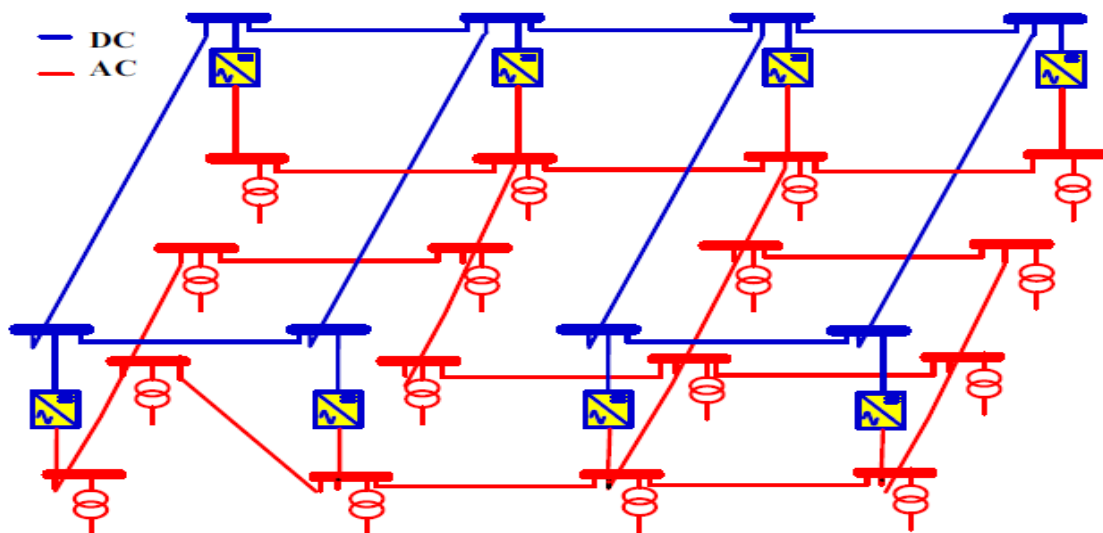


Figure 1. A simple typical representation of an AC overlaid MTDC network [12]

In order to study more precisely the topic of DC systems, we should carefully consider the following issues: mainly, there are two major constraints in using DC resources: first, accessibility to generated electricity (availability), and second, the cost of equipment [17].

Simultaneously, it can be said that DC systems are coming more popular than AC systems owing to their higher efficiency and reliability, and their easy connection to renewable energy resources [18-20]. In addition, in order to reduce fluctuations of power generated in a hybrid system, a battery bank could be used as an energy storage, which absorbs power surplus and power supply shortages in working conditions.

Recently, in order to promote power quality and energy output, smart DC microgrid proposed by some experts. They conclude that modern electrical loads and scattered energy resources are DC type inherently using DC microgrids prevented from added translational AC/DC or DC/AC. On the one hand, some researchers recommended stability analysis in hybrid AC-DC microgrid to achieve higher energy output. Overall, a hybrid microgrid combined of two components: DC component and AC component. Scattered energy resources and DC inherent loads connected to DC component and inherent AC resources and loads linked to AC component. For power quality optimization, energy storage like batteries might connect to DC components.

On the other hand, system stability plays a significant role in microgrid systems. In this regard, in the references [21, 22], hybrid microgrid composed of wind turbine, PV unit, and AC and DC loads are simulated using MATLAB software. Considering solar and wind instability features, control plans designed for invertors so that preserve stability performance of hybrid microgrid. Similarly, for electric vehicles (EVs), the authors of the papers [23, 24] proposed a battery-ultra-capacitor in Hybrid Energy Storage System (HESS).

Another issue of interest in microgrid is their islanding states. In this case, serious and necessary controls should be considered in the various fields of protection and security of microgrid. Herein, in order to minimize the power loss in hybrid AC/DC microgrid systems by optimizing the output power of Renewable Energy Distributed Generators (REDG), the authors of paper [25] presented a Hybrid Nelder-Mead and Cuckoo Search (HNMCSS) algorithm. A typical diagram of the modelled system is displayed in the Figure 2 where the islanded hybrid microgrid system is displayed with AC and DC sub grids.

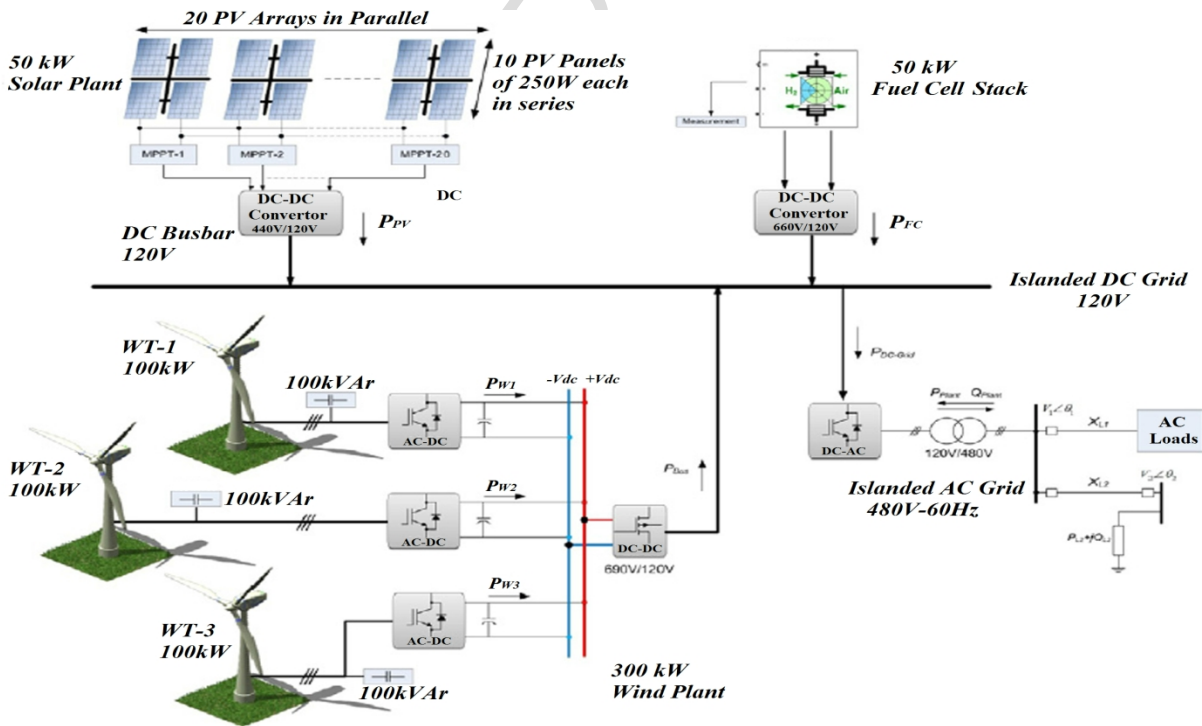


Figure. 2. A typical diagram of islanded hybrid microgrid [25]

Traditionally, converters use a two-stage AC/DC/AC system to convert the input AC voltage and current to the variable frequency and/or the variable amplitude. This kind of instrumentation yields the need for bulky DC-link storage such as electrolytic capacitor [26]. In recent years, most of the microgrids accept conventional AC grid systems; thus, the distributed energy resources need some form of power converters to transfer and convert power from these energy resources to the AC grid system. For instance, wind turbines require back-to-back power converters to synchronize and adjust the output frequency and voltage level with the AC grid system [27, 28]. In this regard, S. Jain, M. B. Shadmand, and R. S. Balog in the reference [29] presented an auto-tuning method for online selection of the cost function weight factors in Model Predictive Control (MPC), where in this paper, a forecasting power control algorithm which decouples active and reactive power for grid integration of PV systems using a quasi-Z-source inverter was proposed. The structure block of a typical smart AC microgrid system including RESs (wind turbine and solar PV), EVs, AC loads, Energy Storage System (ESS) (flywheel, uninterruptible power Supply (UPS), and battery bank), household appliances (PC, cell phone, and fan), AC–DC converters, communication protocols, and Central Processing Unit (CPU) are shown in Figure 3.

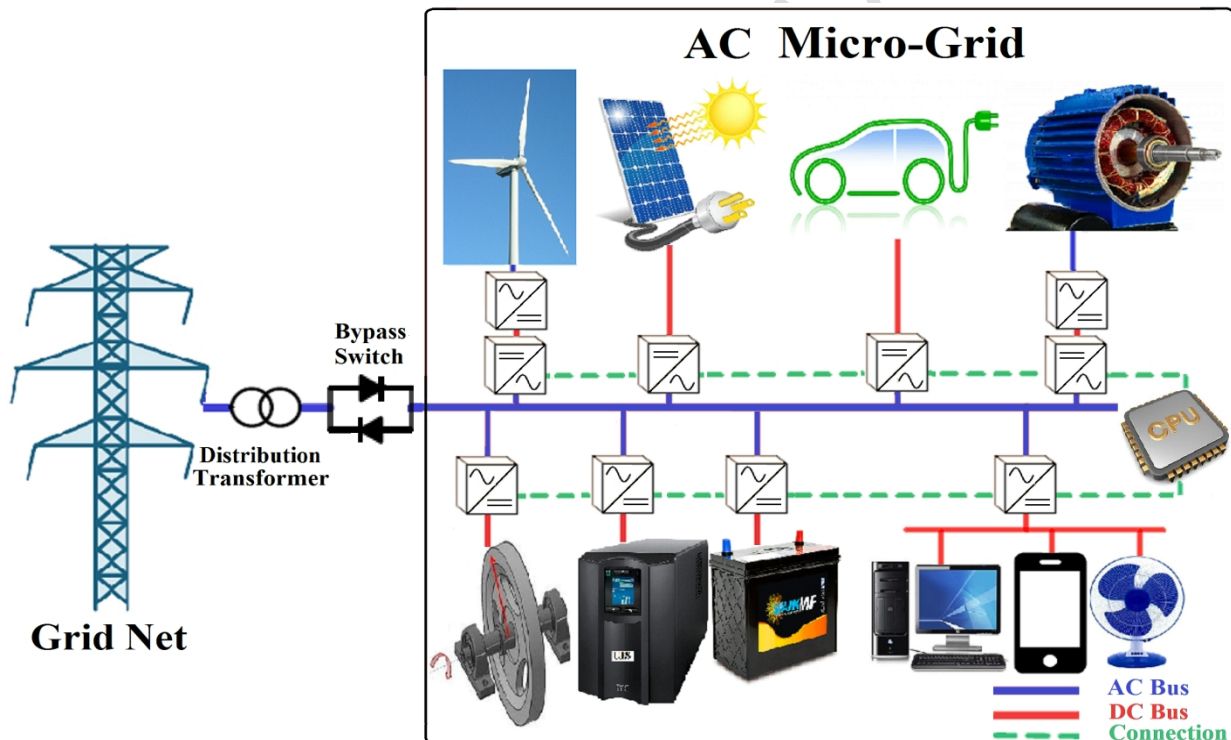


Figure 3. Structure block of a typical smart AC microgrid system

In addition, as a result of recent advancement in design of EVs, the impact of their connections to the Low Voltage (LV) distribution systems is considerably increased. Similarly, in industrial environments, a number of adjustable speed AC drives are utilized, which also need AC/DC and DC/AC converters. In commercial and residential areas, grid connected equipment including computers, battery chargers, and high efficient lighting systems use DC power. Therefore, these equipment need an AC/DC converter to be jointed to the AC grid. These multiple conversion stages reduce the overall reliability and efficiency of the systems. Some of these conversion

stages can be reduced or replaced by a high efficient DC/DC converter if these devices are directly jointed to a DC grid. The structure block of a typical DC microgrid system including RESs, EVs, AC loads, and energy storage system, household items, AC-DC converters, communication protocols and CPU are shown in Figure 4.

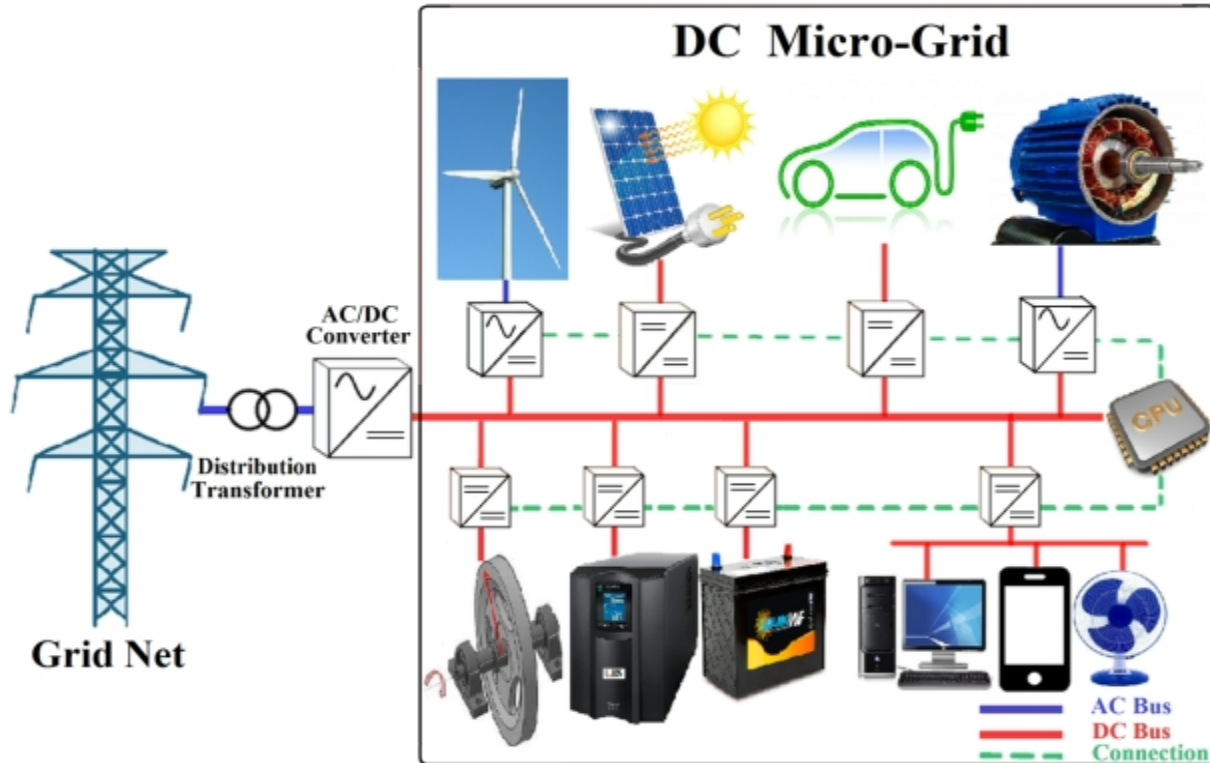


Figure 4. Structure block of a typical smart DC microgrid system

As can be seen from the Figure 4, in a DC microgrid system, the power electronic loads and energy resources can be supplied more efficiently and effectively by opting appropriate voltage level; consequently, it prevents a few stages of conversion. Besides, the ESS can be straightly jointed to the main DC bus or jointed using a DC/DC converter.

Also, it can be said that each approach would have some positive and negative advantages and disadvantages that depend on their requirements and applications. For instance, every battery bank system has not-stable output voltage, and their variations in the output voltage depend on some issues such as battery configuration, battery chemistry; materials, ambient temperature, current, and State of Charge (SoC). The straight connections of battery bank to the DC bus could bring about fluctuation in the voltage of bus and inrush current, and also can lead to shortening the lifetime of the batteries. Furthermore, the fluctuating of the DC voltage can make protection and stability problems in every DC grid system. Therefore, these kinds of converters (DC/DC) are usually recommended for interfacing battery bank systems to the DC bus [27, 30, 31].

In order to introduce Multi-Objective Particle Swarm Optimization (MOPSO) algorithm, it should be noted that, the MOPSO algorithm was introduced by Carlos A. Coello in 2004; in fact, this algorithm is an improved version of the PSO algorithm which is used to solve multi-objective problems [32]. PSO is a metaheuristic approach in Artificial Intelligence (AI) which can be used to find approximate solutions to extremely difficult or impossible problems [26, 33].

### 1.3. Paper Structure

The rest of this paper is organized as follows: energy management requirements are stated in Section 2; materials and methods (optimization of the photovoltaic - wind system) are fully introduced in Section 3; the structure of the grid (study case) is presented in Section 4; the numerical analyses and results of simulations are discussed in Section 5; and finally we provide conclusion in Section 6.

## 2. Energy Management Requirements

One of the most important issues in the study of renewable energy resources would be the issue of energy management. Power converters and Energy Management Algorithm (EMA) together provide the essential control to the system [34]. Photovoltaic panel and Wind Turbine Generator (WTG) can be controlled to extract maximum power from the available natural resources. Furthermore, energy storage system needs management for deciding which storage have to be used in case of a hybrid energy storage system; also, for deciding the charge-discharge cycles of chosen storage.

Another item that needs to be noted in a DC microgrid is that the DC-link voltage should be stable constant for balanced flow of energy among the multiple loads and resources. In addition, based on [35], a variation of DC-link voltage would disrupt the system's normal operation, and also could bring about the whole system to collapse. As can be seen in the reference [22], equations (1) and (2) provide the generalized stability criteria for some microgrids.

$$\frac{P_m - P_e}{\omega} = J \frac{d\omega}{dt} \quad (1)$$

$$P_{load}(t) \leq P_g(t) \pm P_s(t) \quad (2)$$

where  $P_m$  is the wind turbine mechanical power (W);  $P_e$  defines as a wind turbine electrical power (W);  $J$  defines as a inertia ( $\text{kg.m}^2$ );  $\omega$  is WTG speed (rad per sec);  $P_{load}(t)$  defines as an instantaneous load power (W);  $P_g(t)$  defines as total instantaneous power of generating sources (W); and  $P_s(t)$  defines as total instantaneous power delivered by ESS (W)

## 3. Materials and Methods: Optimization of the Photovoltaic - Wind System

In this section, first, the objectives of the system are expressed mathematically, and then in the following sections, the optimization results are described. The power produced by wind and photovoltaic generators for feeding the DC bus is most important and if the power is insufficient, the battery should be discharged to a certain extent to feed the DC bus. If there is not enough power again, it can be purchased a certain amount of power from network. Therefore, the input power of the network has the least priority.

### 3.1. Costs

One of the most important issues of industrial development is currently the cost issue. The cost functions of renewable energy technologies including fuel cells wind and power plants are modeled by linear functions in the reference [36]. Besides, the proposed approach in the reference [37] has determined the optimum weight factors of the cost function for each sampling time; the optimization of the weight factors was done according to the prediction of the absolute tracking error of the control objectives and the corresponding constraints. The bulk of the system costs include the price of photovoltaic panels, wind turbines and battery banks. Based on the

reference [17], the total cost of the system, based on (dollars (\$) per year), includes the purchase of equipment, operation and maintenance, which can be stated as follows;

$$\text{Cost} = C_{\text{Network}} + \frac{\sum_{i=\text{Wind; Photovoltaic; Battery}} (C_i + M_i O)}{N} \quad (3)$$

where: in the equation (3),  $C_i$  and  $M_i O$  are the initial cost, and the cost of operating and maintenance of each component, respectively.  $N$ ,  $C_{\text{Network}}$ , and  $\text{Cost}$  represent the lifetime of the system, the cost of power input from the network, and the total system cost per dollar per year, respectively. Therefore, the first objective function (OF) is formulated as follows;

$$OF_1 = \text{Min}_{\text{Cost}} (A_{\text{Wind}}, A_{\text{Photovoltaic}}, P_{\text{Battery}}, \hat{\rho}) \quad (4)$$

$A_{\text{Wind}}$ ,  $A_{\text{Photovoltaic}}$ ,  $P_{\text{Battery}}$ , and  $\hat{\rho}$  also represent surface area of the winding for the turbine, panel surface, bank capacity of the battery, and ratio of input power from the network to the load. The initial purchase, operation, and maintenance costs for the photovoltaic subsystem are as follows:

$$C_{\text{Photovoltaic}} = \alpha_{\text{Photovoltaic}} \times A_{\text{Photovoltaic}} \quad (5)$$

$$OM_{\text{Photovoltaic}} = OM_{\text{yearly}} \times A_{\text{Photovoltaic}} \times \sum_{i=1}^N \left( \frac{1+\nu}{1+\gamma} \right)^i \quad (6)$$

here:, respectively. Besides,  $C_{\text{Photovoltaic}}$  and  $OM_{\text{Photovoltaic}}$  are symbol of the initial cost and total cost of operation and maintenance of the photovoltaic subsystem;  $\alpha_{\text{Photovoltaic}}$  also indicates the cost of the solar panel which will be given in case study.

Initial costs, operation and maintenance for the wind system are also expressed in the same way in the Equations (7) and (8), respectively.

$$C_{\text{Wind}} = \alpha_{\text{Wind}} \times A_{\text{Wind}} \quad (7)$$

$$OM_{\text{Wind}} = OM_{\text{yearly}} \times A_{\text{Wind}} \times \sum_{i=1}^N \left( \frac{1+\nu}{1+\gamma} \right)^i \quad (8)$$

Similarly;  $OM_{\text{yearly}}$ ,  $\nu$ , and  $\gamma$  respectively represent the annual operating and maintenance cost of each unit, the escalation rate and the interest rate for wind system, respectively. Moreover,  $C_{\text{Wind}}$  and  $OM_{\text{Wind}}$  are the symbol of the initial cost and total cost of operation and maintenance of the wind subsystem;  $\alpha_{\text{Wind}}$  also indicates the cost of the wind turbine which will be given in case study.

In addition, initial costs, operation and maintenance for the battery bank are also expressed as follows:

$$C_{\text{Battery}} = \alpha_{\text{Battery}} \times P_{\text{Battery}} \quad (9)$$

$$OM_{\text{Battery}} = OM_{\text{yearly}} \times P_{\text{Battery}} \times \sum_{i=1}^{T_B} \left( \frac{1+\nu}{1+\beta} \right)^{(i-1)N_{\text{Battery}}} \quad (10)$$

where in the equations (9) and (10):  $OM_{\text{yearly}}$ ,  $\nu$ ,  $\beta$ ,  $C_{\text{Battery}}$ , and  $OM_{\text{Battery}}$  represent the annual operating and maintenance cost of each unit, escalation rate, inflation rate, symbol of the initial cost and the total cost of operation and maintenance for the battery system, respectively;  $\alpha_{\text{Battery}}$  also indicates the cost of the battery bank which will be given in case study.

Since in industry, the battery lifetime is less than solar cells and wind turbines, they are expected to be replaced several times over the lifetime of the system. Thus, the last part of the equation

(10) is used to express the replacement cost as the cost of operation and maintenance. The cost of power input from the network is formulated as the following equation;

$$C_{Network} = \sum_{i=1}^T P_{Network,t} \times \alpha_{Network} \quad (11)$$

where  $P_{Network,t}$  indicates the power purchased from the network in each unit, and  $\alpha_{Network}$  also indicates the cost of input power from the network according to the reference [17]. The amount of  $P_{Network,t}$  and  $\alpha_{Network}$  will be given in case study.

### 3.2. Availability and Reliability

When energy is accessible, availability is presented as an important indicator for the system. There is an important difference between availability and reliability. Availability is the ability of the system to provide power to the load, and reliability is the system's ability to operate without failure. A highly reliable photovoltaic system, in which components fail, can have little availability, provided that there is enough energy to supply the required load overnight or cloudy days. A certain level of availability can be achieved with many system settings. According to the reference [17], typically the availability for the intended duration is formulated as follows;

$$A = 1 - \frac{\Delta P}{D} \quad (12)$$

where  $D$  is early demand, and demand not met ( $\Delta P$ ) can be explained as Equation (13):

$$\Delta P = \sum_{t=1}^T (P_{Battery_{Min}}(t) - P_{Battery_{SOC}}(t) - (P_{Photovoltaic}(t) + P_{Network}(t) + P_{Wind}(t) - P_D(t)) \times U(t)) \quad (13)$$

Here, if the power supply is greater or equal to the demand, a step function is zero, and if the demand is not met, it is assumed to be 1. The parameters  $A$ ,  $\Delta P$ ,  $P_{Battery_{Min}}(t)$ ,  $P_{Battery_{SOC}}(t)$ ,  $P_D(t)$ , and  $U(t)$  indicate availability index, demand not met in kilowatt-hours per year (kWh/y), minimum charge of the battery bank in time, battery charge status in time, amount of demand in time unit, and step function, respectively. Herein, the input powers of the network are given as:

$$P_{Network} = \partial \times (P_D(t) - P_{Photovoltaic}(t) - P_{Wind}(t) - P_{Battery}(t)) \quad (14)$$

$$P_{Wind} = P_{WTG} \times A_{Wind} \times \eta_{Wind} \quad (15)$$

$$P_{Photovoltaic} = Insolation \times A_{Photovoltaic} \times \eta_{Photovoltaic} \quad (16)$$

In equations (12) to (14),  $P_{Photovoltaic}$ ,  $\eta_{Photovoltaic}$ ,  $Insolation$ ,  $P_{Wind}$ , and  $\eta_{Wind}$  represent the efficiency of the photovoltaic subsystem, the amount of sunlight to the cell surface, the turbine power subsystem, and the efficiency of the wind turbine subsystem, respectively. Also  $P_{WTG}$  is the power of wind turbine generator which will be given in case study.

The second objective function can be expressed as follows:

$$OF_2 = Max_A (A_{Wind}, A_{Photovoltaic}, A_{Battery}, \partial) \quad (17)$$

### 3.3. Optimization

#### 3.3.1. Design limitations

A physical limitation which has to be added to the optimization algorithm is the area that can be used to install and set up solar panels. Formula (18) shows these surface limitations.

$$A_{Photovoltaic_{Min}} \leq A_{Photovoltaic} \leq A_{Photovoltaic_{Max}} \quad (18)$$

These limitations also need to be considered for wind turbine that is given in equation (19).

$$A_{Wind_{Min}} \leq A_{Wind} \leq A_{Wind_{Max}} \quad (19)$$

Certainly the lower bound limitation can be zero, but based on [38], in order to increase the reliability of the system, the lower bound for a wind turbine is considered at least 100 m<sup>2</sup>. The input power of the network should also be within the range below:

$$P_{Network_{Min}} \leq P_{Network} \leq P_{Network_{Max}} \quad (20)$$

Part of input power from the network can be changed in the range of zero and one which is shown in the equation (14).

Finally, in order to avoid excessive enlargement of the system followed by the addition of excessive costs, the total production capacity of power should not be greater than the amount of demand, which is shown in equation (21).

$$P_{Wind}(t) + P_{Photovoltaic}(t) + P_{Battery}(t) + P_{Network}(t) \leq P_D(t) \quad (21)$$

### 3.4. Principles of Multi-objective particle swarm optimization and PSO algorithms

In the multi-objective particle swarm optimization algorithm, a concept called ‘Archive’ (Repository) has been added to the single-objective particle swarm optimization algorithm. Choosing the best overall answer and the best personal response for each particle is an important step in the MOPSO algorithm. When particles want to make a movement; they select a member of the archive as a leader. This leader must be a member of the archive. Archive members represent Pareto-Front and include non-dominated particles, which will be discussed later on. Then instead of  $G_{best}$ , one of the members of the archive is chosen. Since there is only one target and particle in the single-objective algorithm, and this particle is the best one, there is no archive in the single-objective algorithm, but in the multi-objective algorithm, there are several particles that are non-dominated and are in the set of answers.

In order to compare the best personal response, the following applies:

If the new position dominates the best answer, new position replace with the best answer; in mathematical terms:

$$P_{best_i}^{n+1} = X_i^{n+1} \quad (22)$$

If the new position is dominated by the best response, nothing will be done. In mathematical terms:

$$P_{best_i}^n = P_{best_i}^{n+1} \quad (23)$$

If none of them dominates one another, one of them will randomly take as the best position. In the Figure 5, several samples Front using epsilon dominance found by MOPSO is shown.

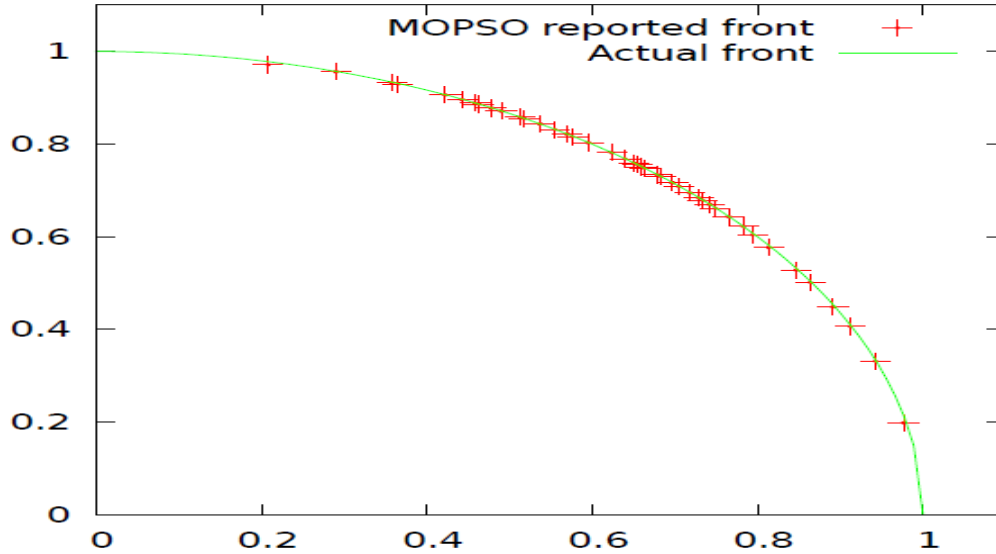


Figure 5. several samples Front using epsilon dominance found by MOPSO

The proposed algorithm can be readily applied according to the following steps:

1- Determining and gathering the parameters required for the implementation of the MOPSO includes: maximum repetition for execution of the algorithm, population size, C1 and C2 values, and archive volume.

2- Initial population is created.

3- Apply the load flow algorithm to the generated population.

4- The best individual response to each particle is determined.

5- Non-dominated members are separated and stored in the archive.

6- Each particle among the members of the archive selects a leader and performs his own movement (speed and position is updated).

7- The best individual responses to each particle are updated.

8- New non-dominated members are added to the archive.

9- Dominated members of the archive are removed.

If the termination conditions are not met, the algorithm is repeated from step 6.

10- Investigate the stop conditions.

11- Select the best interactive solution.

Figure 6 shows multi-objective particle swarm optimization algorithm for the proposed hybrid system.

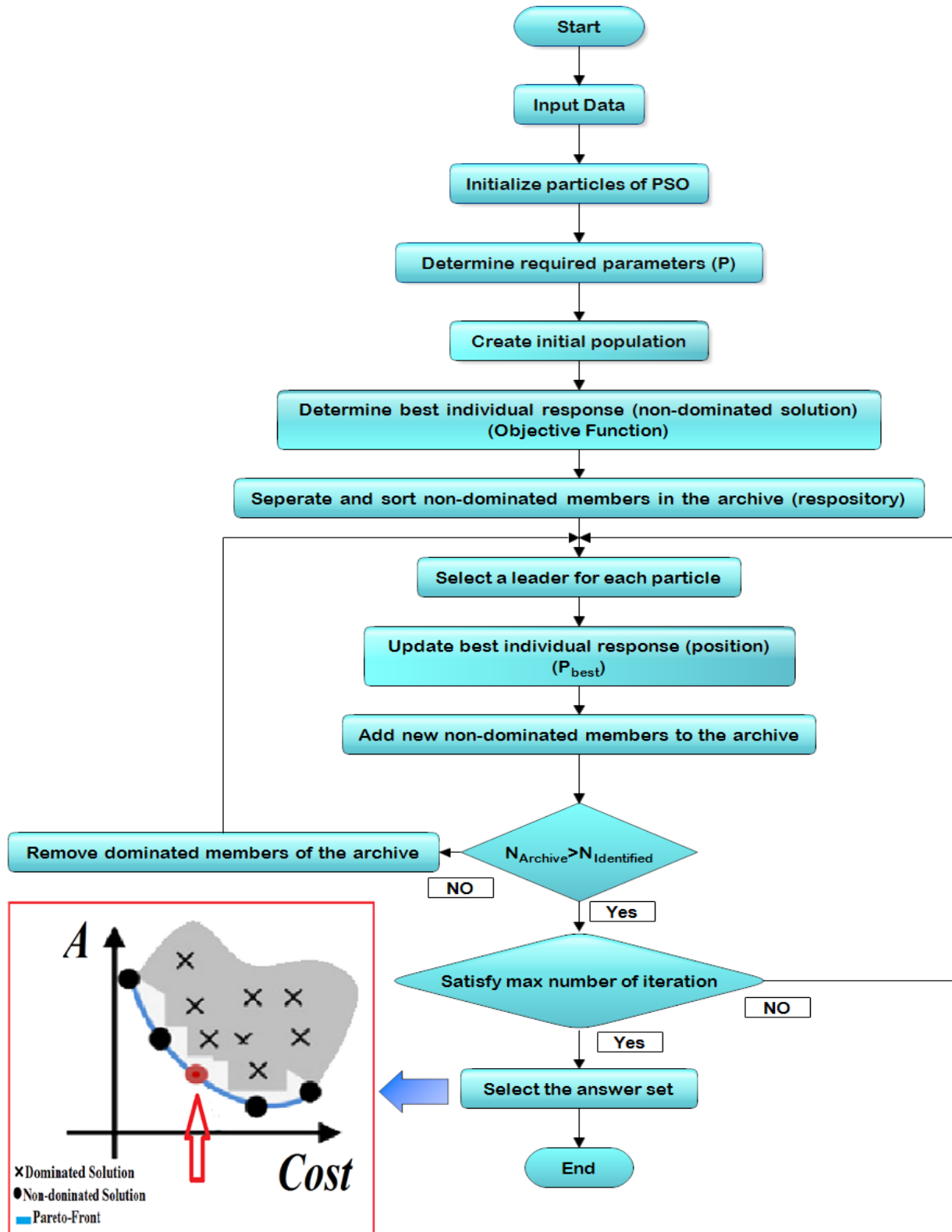


Figure 6. Multi-objective particle swarm optimization (MOPSO) algorithm for the proposed hybrid system

The important difference between single-objective and multi-objective particle swarm optimization is that in the case of multi-objective optimization, there may be several solutions that can meet the goal of optimization; if this method is not influenced by any of the other techniques, it will be recognized as a superior technique.

### 3.5. Selection of particle elements for design

In order to design a multi-objective hybrid (photovoltaic, wind, battery bank) system, considering equations (3) and (4), the desired particles are selected considering the following equation;

$$Particles : A_{Photovoltaic} ; A_{Wind} ; P_{Battery} ; \partial \quad (24)$$

#### 3.5.1. Data and conditions to be used in optimization

Using equations (4) and (14), the multi-objective cost function is expressed and equations (18) to (21) also specify the problem constraints.

The variables reviewed in this article are as follows:

d: the number of variables in the cost function (algorithm dimension),

n: represents the population (number of particles),

N: the highest number of repetitions,

C1 and C2: learning factors,

$\omega_1$  and  $\omega_2$ : primary and secondary inertia factors,

In spite of these variables, MOPSO calculates  $G_{best}$  across the population by optimizing the amount of interest by taking a value for error rate; therefore, by identifying the parameters of the algorithm, the cost function can be minimized.

### 3.6. Multi Objective Genetic Algorithm (MOGA)

According to the references [17, 39, 40], multi objective genetic algorithm or (MOGA) which is usually titled “non-dominated sorting genetic algorithm-II” or (NSGA-II) is utilized as a search method or an optimization algorithm to find a set of correct solutions as a form of Pareto frontier. In order to achieve good result in multi-objective optimization, MOGA utilizes genetic algorithm (GA) as its core with two main concepts including crowding distance and non-dominated sorting. Multi objective genetic algorithm is briefly expressed in this paragraph. In iteration phase  $t$ , child’s population  $Q_t$  and parent population  $P_t$ , each of them with  $N$  solutions, are mixed to form a greater population with  $2N$  solutions; then, to find solutions, non-dominated sorting is carried out with similar ranks. After that, sorting process is carried out by choosing solutions with the lowest rank, then, solutions with the next lowest rank, and it will be continued; until the number of solutions in the parent population exceeds  $N$ , this procedure continues. After that, for the latest sorted sub-population contained in the parent’s population, as long as the parent’s population finds the exact  $N$  solutions, just the solutions with a greater crowding distance are opted. Then, mutation operators and crossover are carried out to find the next child population. In this paper, for optimizing the hybrid system, the flowchart of NSGA-II algorithm is used which is given in the Figure 7.

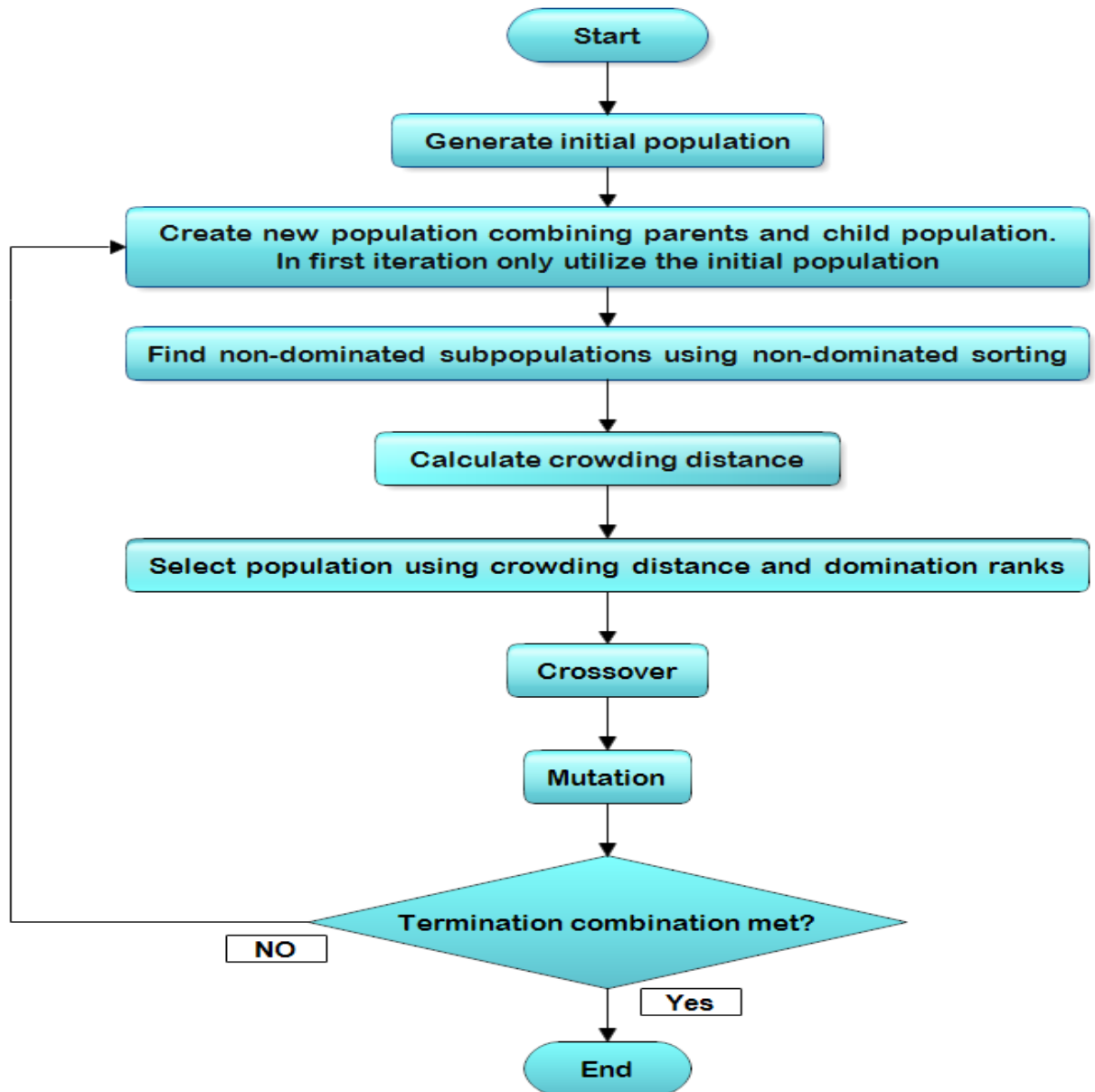


Figure 7. Flowchart of NSGA-II algorithm

Furthermore, in this study, the proposed MOPSO algorithm to the microgrid is applied. Herein, in order to demonstrate the efficiency and possibility of the proposed method, the optimization problem is designed and implemented in two Scenarios:

- (1) Main operation (*Basic Scenario*) which represents the normal function of the grid.

The main objectives in this paper are the cost and availability. Thus, a function have to be defined which relates each one point in a dimensional objective space to a yield or scalar value. The yield function is given in the equation (25).

$$Y = Cost \ A \quad (25)$$

Then, we should convert all objectives to same scale. In order to optimize the hybrid system, the general form of value function can be given as:

$$Y(Cost, A) = \theta_1 \frac{Cost - (Min(Cost))}{Max(Cost) - Min(Cost)} - \theta_2 \frac{A - (Min(A))}{Max(A) - Min(A)} \quad (26)$$

In equation (26),  $\Theta_1$  and  $\Theta_2$  are the weighing ratios which can be defined by designer. In Basic scenario, the assumption is that  $\Theta_1 = \Theta_2$  which means there are no differences between the cost and availability of the hybrid system. Herein, using genetic algorithm optimization toolbox in MATLAB software, by minimizing  $Y(Cost, A)$ , the decisive result on the design variables could be received.

- (2) Operation at the presence of maximum capacity of renewable energy (*Maximum Renewable Scenario*), which demonstrates the use of the maximum generation capacity for photovoltaic and wind units per day.

In the Maximum Renewable Scenario, the assumption is that less weight is given to the cost than availability ( $\Theta_1 = 0.3$ , and  $\Theta_2 = 0.7$ ) in the  $Y(Cost, A)$  function.

#### 4. Structure of the Grid (Study Case)

For the study case, in this paper, we have used a small residential area that includes microgrid with renewable energy resources (wind and photovoltaics) as well as battery bank as energy storage unit with the actual values. Therefore, in the case study, we use high temporal resolution information collected from a 25 kW photovoltaic system installed on residential area; the monthly average load requirement for this residential area is roughly equal to 75 kWh. The technical and economic specifications of the units are provided in Table 1. Besides, the market price offered is displayed in Figure 8. The output power levels of the WT and PV based on the predicted values are provided in Table 2. In this study, we have considered the battery with the capacity of 30 kWh, which amounted to almost 4 kWh after considering the residential feeder with a maximum charging power (230 V/16 A) electrical system. The information for monthly wind speed (average), annual clearness index and the solar radiation (average), and the profile of daily load for the microgrid considered in the study case are given in Figures 9, 1 and 11 respectively.

Table 1. Bids and technical coefficient of the DG resources

Unit	Type	Bid (Cent/kWh)	Cost of Startup/Shutdown (Cent)	$P_{Min}$ (kW)	$P_{Max}$ (kW)
1	Main Turbine	0.46	0.965	6	30
2	Wind Turbine	1.08	0	0	15
3	Photovoltaic	2.58	0	0	25
4	Battery	0.38	0	-30	30
5	Network	-	0	-30	30

Table 2. Predicted values of Photovoltaic and Wind Turbine

Time (h)	Photovoltaic (kW)	Wind Turbine (kW)
1	0	1.79
2	0	1.79
3	0	1.79
4	0	1.79
5	0	1.79
6	0	0.92
7	0	1.79
8	0.2	1.3
9	3.8	1.79
10	7.53	3
11	10.5	8.8
12	11.96	10.5
13	23.95	3.92
14	21	2.37
15	7.79	1.79
16	4.3	1.31
17	0.6	1.79
18	0	1.79
19	0	1.31
20	0	1.79
21	0	1.3
22	0	1.3
23	0	0.91
24	0	0.61

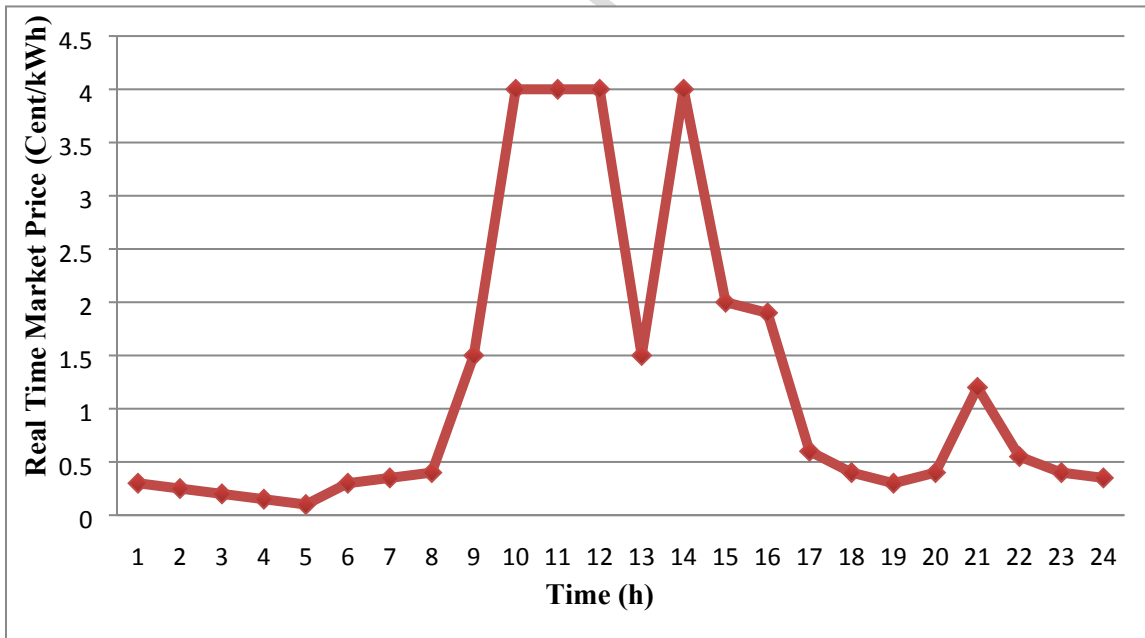


Figure 8. Market price

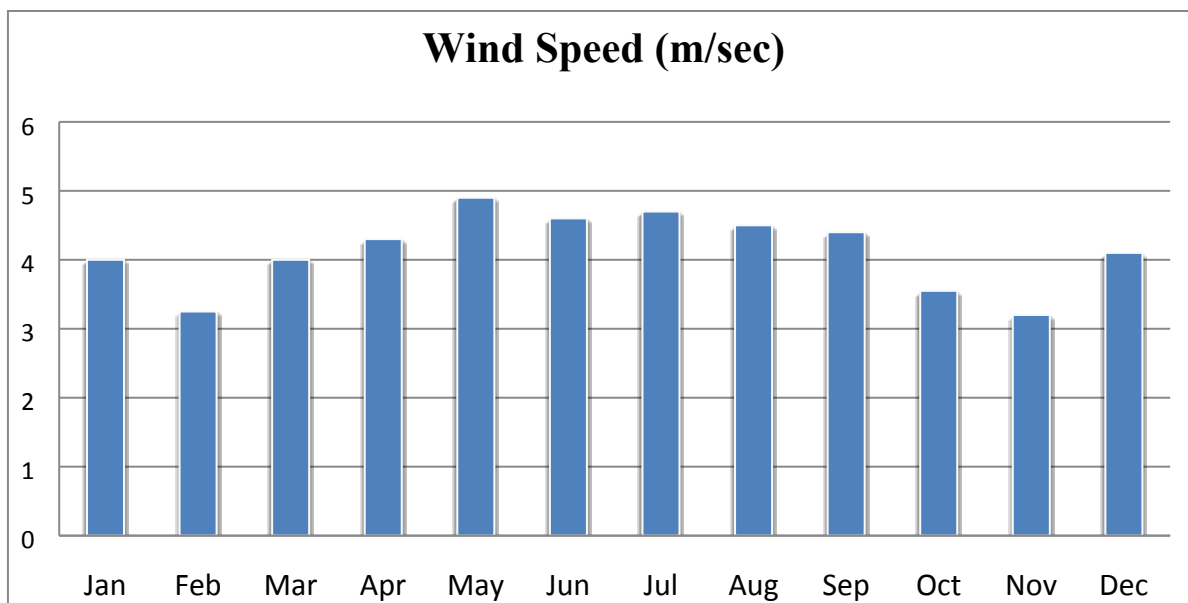


Figure 9. The data for monthly wind speed (study case)

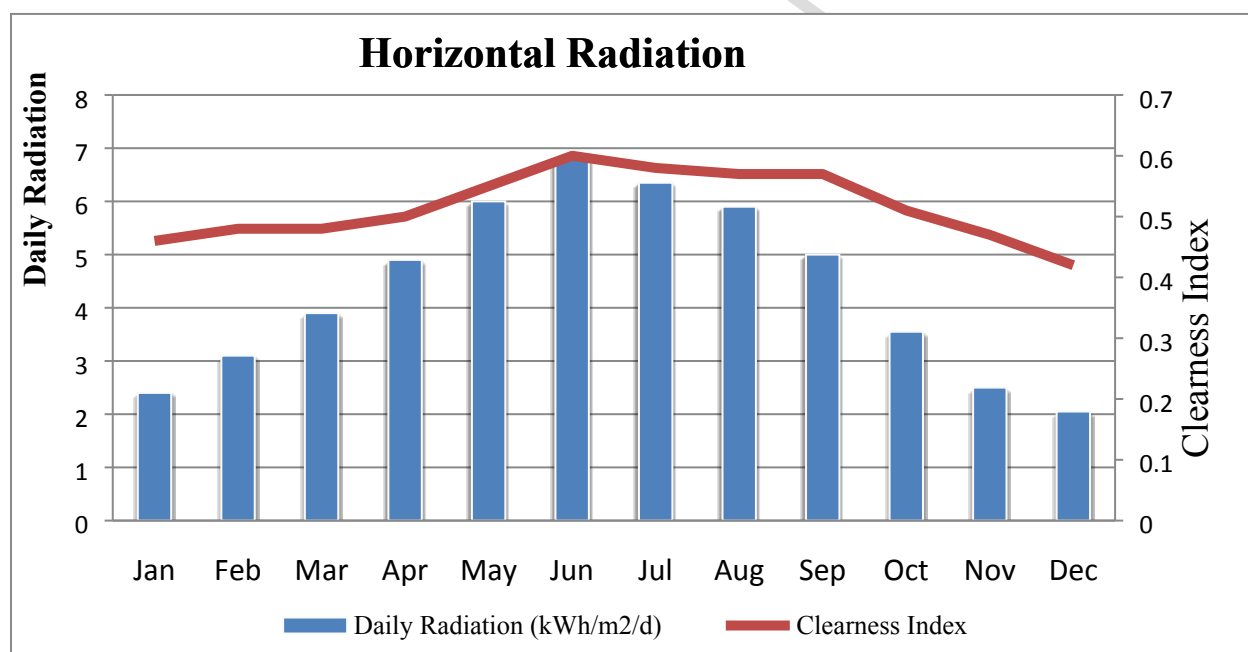


Figure 10. The annual clearness index and the solar radiation for the location of study case

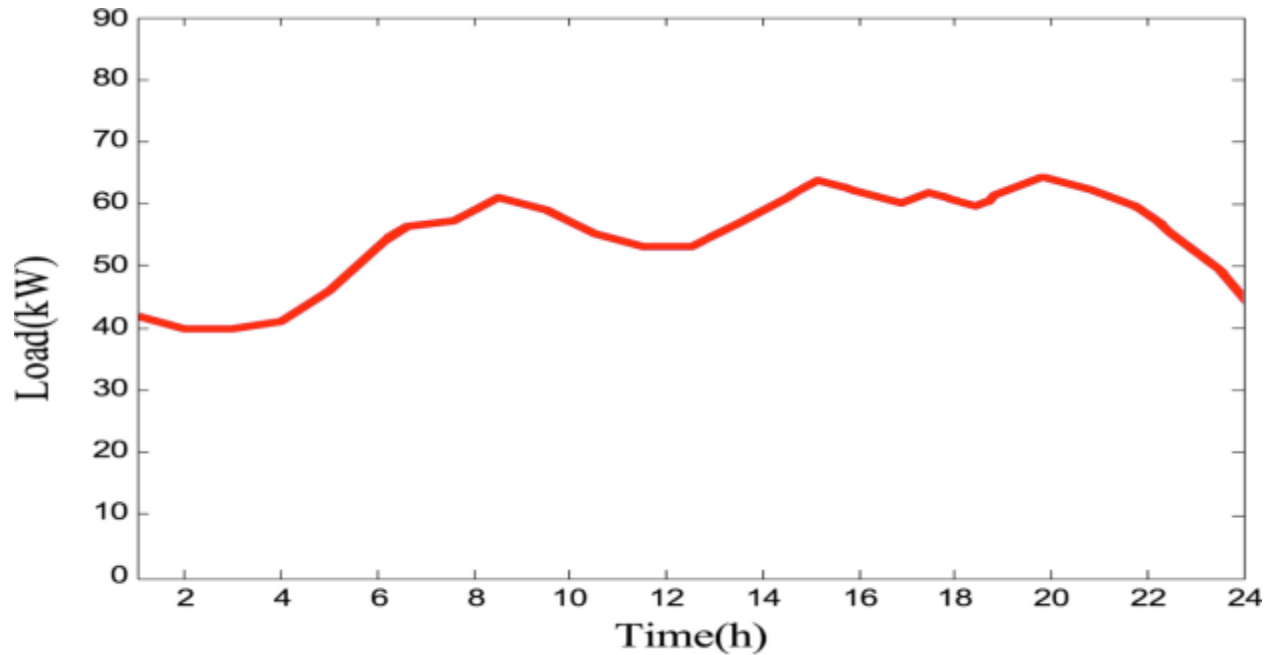


Figure 11. The profile of daily load for the microgrid considered in the study case

In Tables 3 and 4, the numerical information of the hybrid system and the constraints numerical information are given respectively. In this paper, to make the model more realistic, in mathematical simulations, we consider economic aspects such as interest and escalation rates.

Table 3. The numerical information of the hybrid system

Parameters	Information
Lifetime of the plan	20 years
Lifetime of the battery bank	5 years
Escalation rate	10 percent
Interest rate	10 percent

Table 4. Constraints numerical Information

Parameters	Information
$A_{Wind_{Max}}$	4200
$A_{Wind_{Min}}$	100
$A_{Photovoltaic_{Max}}$	4200
$A_{Photovoltaic_{Min}}$	0

The amount of  $\alpha_{Photovoltaic}$ ,  $\alpha_{Wind}$ ,  $\alpha_{Battery}$ ,  $\alpha_{Network}$ ,  $P_{Network}$ , and  $P_{WTG}$  are given in Table 5.

Table 5. Values of  $\alpha_{Photovoltaic}$ ,  $\alpha_{Wind}$ ,  $\alpha_{Battery}$ ,  $\alpha_{Network}$ ,  $P_{Network}$ , and  $P_{WTG}$ 

Parameters	Value
$\alpha_{Photovoltaic}$	450 \$/m <sup>2</sup>
$\alpha_{Wind}$	100 \$/m <sup>2</sup>
$\alpha_{Battery}$	100 \$/kWh
$\alpha_{Network}$	0.1 \$/kWh
$P_{Network}$	0.1 \$/kWh
$P_{WT}$	4 kW

Accordingly, the main constraints of each particle in the study case and considering the equations (18) to (20), (24) and Table 2 are as follows:  $0 \leq A_{Photovoltaic} \leq 4200$ ;  $100 \leq A_{Wind} \leq 4200$ ;  $P_{Network_{Min}} \leq P_{Network} \leq P_{Network_{Max}}$ ;  $0 \leq \partial \leq 1$ .

Table 6 shows the numerical values of the algorithm parameters which are used in the study.

Table 6. Numerical values of the algorithm parameters

Parameters	Values
d	6
n	14
N	100
C1	2
C2	2
$\omega_1$	0.9
$\omega_2$	0.4
Error	1-5

In addition, in order to achieve the specific answers in the loading equations in the power system, load flow should be applied to the network, as well as the determination of the specific contribution of each DG in the grid at different hours. Therefore, power flow has been applied in both scenarios, whereby the contributions of each DG resources are shown in following Tables.

## 5. Simulation Results

In this paper, simulation has been performed for 100 repeated, but in some cases, to complete the simulation, operations are repeated so that at least one of the following occurs as a condition of termination: **A)** The algorithm reaches the maximum number of repetitions (N = 100). **B)** The velocity approaches zero and the optimal answer is obtained.

As mentioned in the section 3.6., the optimization problem is designed and implemented in two scenarios (Basic, and Maximum Renewable). In both scenarios, we assumed that the distribution generations operated at a unit power factor. The distribution of the criterion of MOPSO algorithm for availability and operating costs for the Basic Scenario (1) and Maximum

Renewable Scenario (2) are given in Figures 12 and 13; besides, the convergence characteristic of MOGA algorithm for the Basic Scenario (1) and Maximum Renewable Scenario (2) are shown in Figures 14 and 15 respectively.

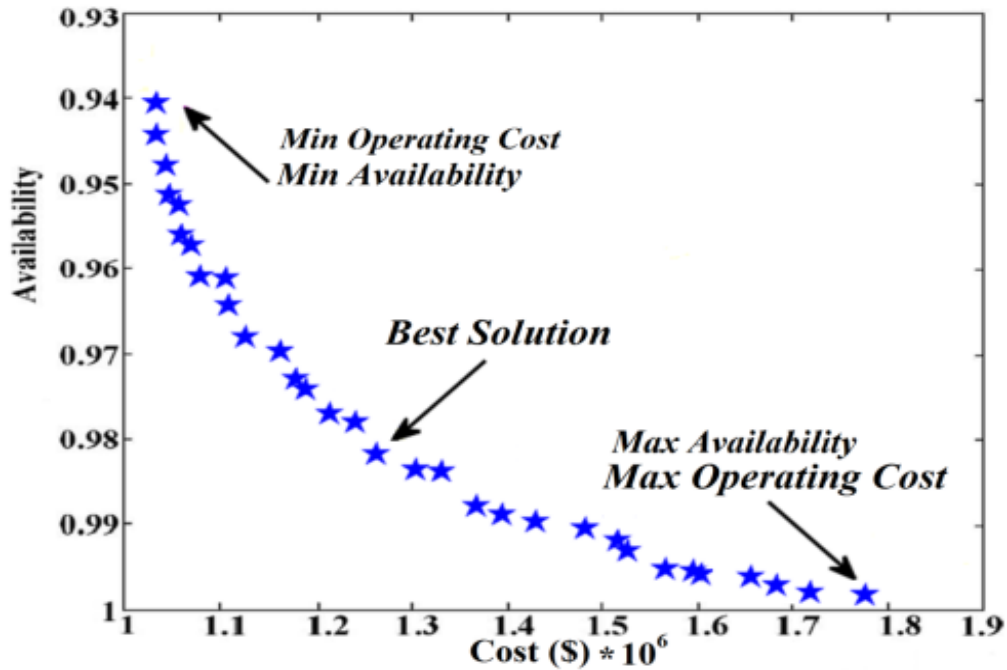


Figure12. Distribution of the criterion for availability and operating costs for the Basic Scenario (1)

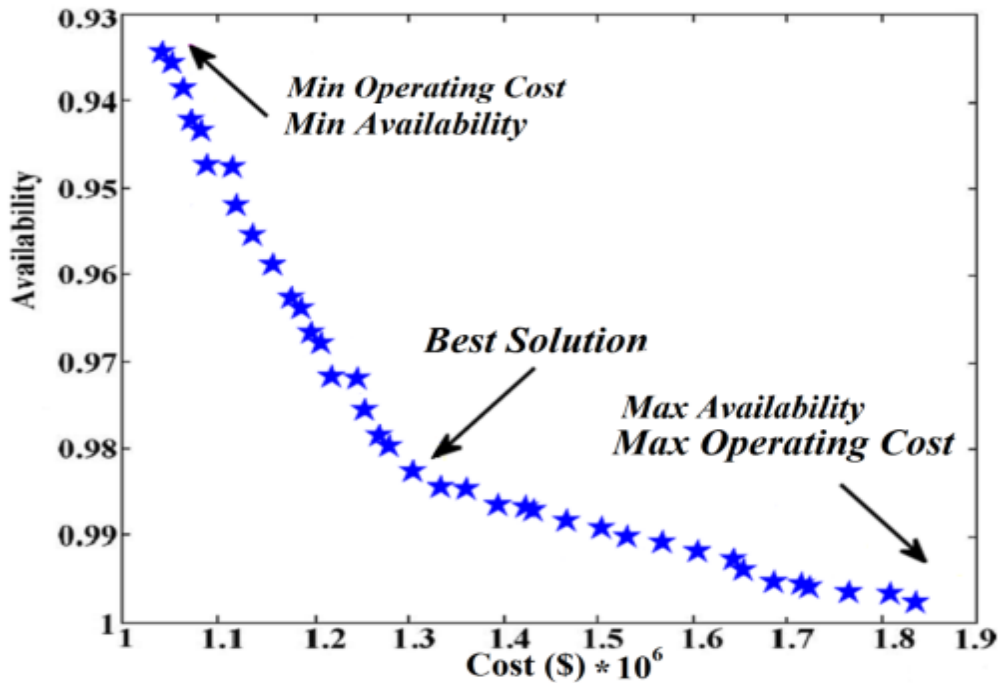


Figure 13. Distribution of the criterion for availability and operating costs for the Maximum Renewable Scenario (2)

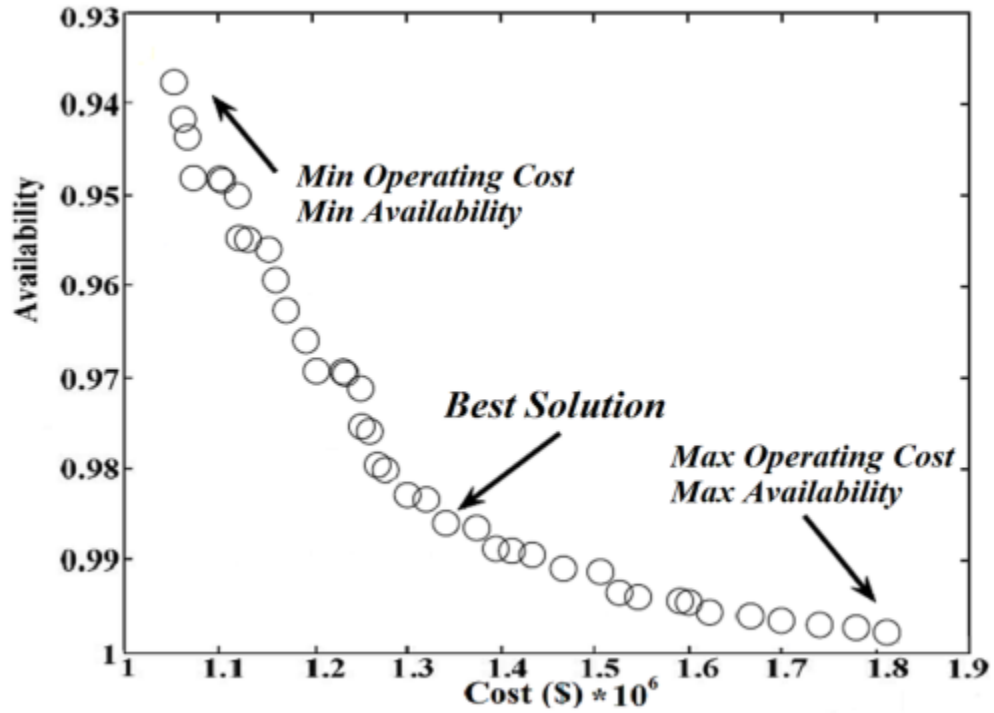


Figure 14. The convergence characteristic of MOGA algorithm for the Basic Scenario (1)

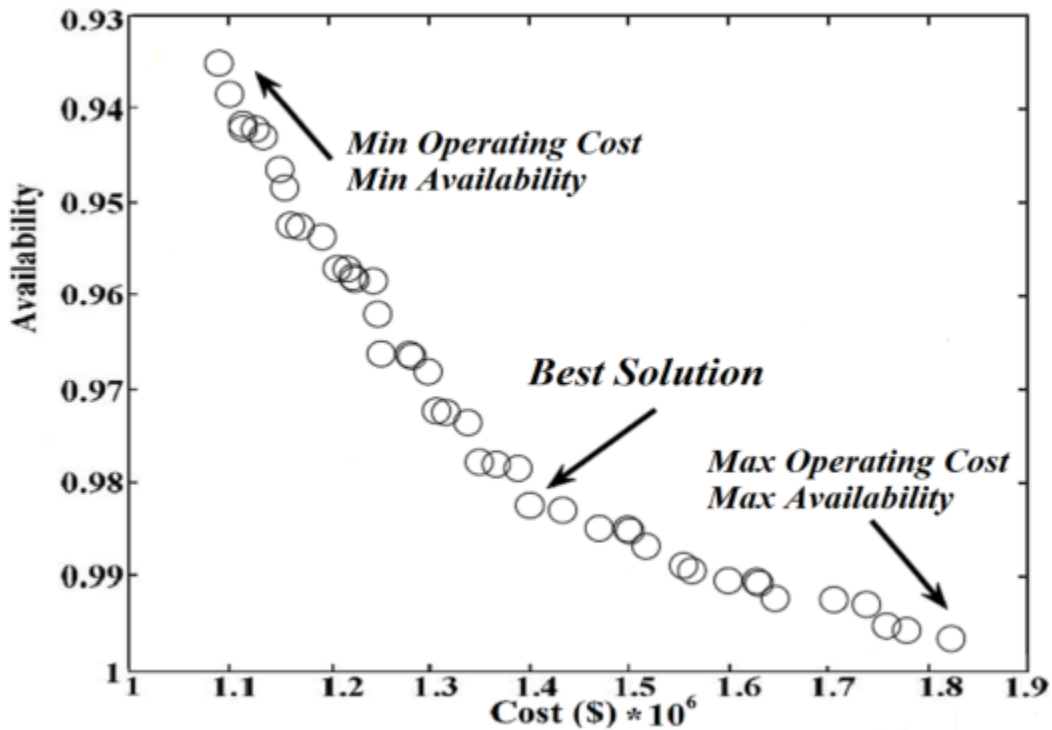


Figure 15. The convergence characteristic of MOGA algorithm for the Maximum Renewable Scenario (2)

Tables 7 and 8 provide the comparison between simulation results for the MOPSO algorithm and MOGA algorithm in both scenarios (Basic, and Maximum Renewable).

Table 7. Comparison for optimized hybrid system design variables for two approaches for Basic Scenario

Approach	$A_{Wind} (m^2)$	$A_{Photovoltaic} (m^2)$	$P_{Battery} (kWh)$	$\partial$	$A$	Costs (\$)
MOPSO	375	2100	245	12.8%	98.35%	$1.252 \times 10^6$
MOGA	360	2900	392	16.9%	98.14%	$1.384 \times 10^6$

Table 8. Comparison for optimized hybrid system design variables for two approaches for Maximum Renewable Scenario

Approach	$A_{Wind} (m^2)$	$A_{Photovoltaic} (m^2)$	$P_{Battery} (kWh)$	$\partial$	$A$	Costs (\$)
MOPSO	710	2860	370	20.5%	98.46%	$1.312 \times 10^6$
MOGA	870	3460	395	26.5%	98.21%	$1.395 \times 10^6$

As can be seen from the Tables 7 and 8, for the Basic Scenario, the operation cost in MOPSO algorithm is decreased by 9.53% compared to MOGA algorithm; the availability, in addition, is increased by 0.21%. For the Maximum Renewable Scenario, operation cost in MOPSO approach is decreased by 5.94% compared with MOGA approach; and the availability is increased by 0.25%. The placement of optimal power considering the operating cost and availability objectives for both Basic and Maximum Renewable Scenarios are shown in Tables 9 and 10 respectively.

Table 9. Placement of optimal power considering the operating cost and availability objectives for Basic Scenario

Hour	Wind Turbine (kW)	Photovoltaic (kW)	Battery (kW)	Yield (kW)
1	0	0	5.47	13.42
2	0	0	-15.48	29.47
3	0.41	0	-10.85	30
4	0.01	0	-13.70	29.74
5	0.50	0	16.45	26.27
6	0.60	0	5.106	23.96
7	0.17	0	12.57	28.42
8	0.43	0.18	14.04	11.42
9	1.72	3.24	30	-17.49
10	3.09	7.52	29.99	-20.61
11	8.37	9.62	30	-30
12	10.42	3.59	30	-30
13	3.91	0	29.89	-21.79
14	2.22	9.66	30	-29.88
15	1.78	7.08	30	-22.65
16	1.30	4.20	29.99	-15.50
17	1.51	0.27	29.99	-6.72
18	0.21	0	14.26	26.13
19	0.40	0	16.80	20.28
20	0.95	0	21.48	10.26
21	1.00	0	29.99	-13.00
22	1.31	0	26.99	-8.86
23	0.43	0	3.63	30
24	0.61	0	-7.57	8.90

Table 10. Placement of optimal power considering the operating cost and availability objectives for Maximum Renewable Scenario

Hour	Wind Turbine (kW)	Photovoltaic (kW)	Battery (kW)	Yield (kW)
1	1.75	0	28.67	-14.69
2	1.79	0	29.99	-16.27
3	1.79	0	30	4.74
4	1.79	0	30	-16.02
5	1.80	0	30	15.21
6	0.91	0	28.65	5.78
7	1.78	0	30	1.79
8	1.30	0.2	29.99	-15.79
9	1.79	3.75	30	-19.53
10	3.00	7.525	30	-20.59
11	8.76	10.45	29.87	-30
12	10.41	11.95	30	-30
13	3.91	23.90	30	-30
14	2.37	21.05	25.06	-30
15	1.78	7.87	30	-23.66
16	1.30	4.22	29.99	-15.53
17	1.77	0.55	30	-7.33
18	1.77	0	30	-3.78
19	1.30	0	30	-1.302
20	1.77	0	29.99	-4.78
21	1.30	0	29.99	-13.30
22	1.30	0	30	-20.30
23	0.91	0	30	-5.48
24	0.61	0	29.99	-10.61

According to the results of simulation, in the first scenario (Basic), in the first hours of the day, most load of the microgrid was supplied by the network, and therefore owing to the peak load, the DGs rose their generation based on the priority requirements of the maximum availability and minimum costs. In order to achieve better economic performance operation, on the other hand, getting energy from the network was replaced with giving energy by the microgrid in the rush hours. In addition, in the early hours of the day, battery charging in the microgrid happened while discharging happened later in the day.

For the second scenario (Maximum Renewable), based on the obtained results, the maximum use of PV and wind units with high Availability and low costs reduced the operating costs moderately for the microgrid compared to the first scenario, but the Availability rate was increased minimally.

As can be seen from the obtained results of the simulation, in order to demonstrate the possibility and effectiveness of MOPSO algorithm, the results are compared to those of multi objective genetic algorithm (MOGA) or NSGA-II. Although, according to Figures 10 to 13, it can be stated that MOPSO algorithm has better performance and proficiency in finding the optimal interaction point between availability and operational cost in both scenarios, compared to MOGA algorithm. Tables 5 and 6 confirm the results of those comparisons. Also, the demand not met can be further decreased by adjusting the weight ratio of cost and availability in the yield function.

It can be said that without loss of generality, the models of the various components, such as wind turbines, photovoltaic panels, and power electronics interfaces can be made arbitrarily complex to ameliorate the constancy of the model. In a wind - photovoltaic hybrid energy system, there are several factors that help to the overall conversion proficiency and efficiency. Taking all the

material mentioned in previous discussions into account, a detailed plan, design procedure, and flowchart of the hybrid system for a smart microgrid is presented in Figure 16.

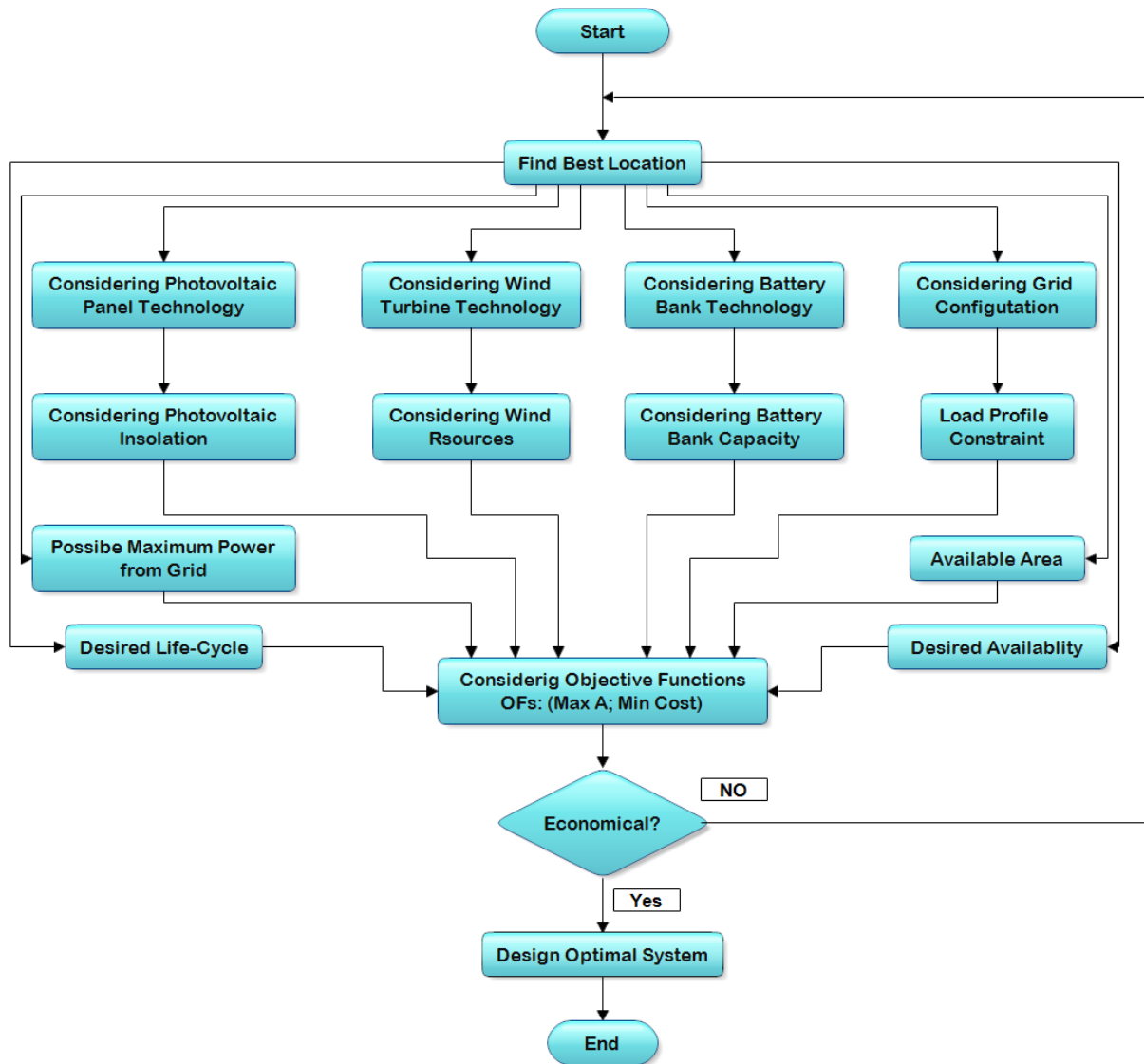


Figure 16. Detailed plan, design procedure, and flowchart of the hybrid system for a smart microgrid

## 6. Conclusion

Generally, at design phase of hybrid renewable energy systems, there are two basic constraints: first, availability, and second, the cost of equipment. Considering these constraints and using DGs as renewable energy resources (RES) including wind turbines and photovoltaics, in this paper, first, a comprehensive analysis on new structures of AC and DC systems was provided, then, using DGs as RESs such as WTs, PVs, and also battery banks as power backup unit and energy storage of the hybrid system, an intelligent method based on MOPSO was used. Moreover, in order to increase the availability and reduce network costs, an optimal design with hybrid RESs in a smart microgrid was proposed. In order to demonstrate the possibility of proposed method, an optimized method was designed and implemented in Basic and Maximum Renewable scenarios.

In Basic Scenario, the operation cost in MOPSO algorithm was decreased substantially by 9.53% compared to the MOGA algorithm; in addition, the availability of the system is increased marginally by 0.21%. Also, for the Maximum Renewable Scenario, operation cost in MOPSO approach was decreased by 5.94% compared with MOGA approach; and the availability was increased minimally by 0.25%. By comparing the proposed method with multi-objective genetic algorithm (MOGA), it is obvious that the proposed method provides a better response.

## References

- [1] T. Dragicevic, J. C. Vasquez, J. M. Guerrero, and D. Skrlec, "Advanced LVDC Electrical Power Architectures and Microgrids: A step toward a new generation of power distribution networks," *IEEE Electrification Magazine*, vol. 2, pp. 54-65, 2014.
- [2] A. Abdolahi, J. Salehi, F. Samadi Gazijahani, and A. Safari, "Probabilistic multi-objective arbitrage of dispersed energy storage systems for optimal congestion management of active distribution networks including solar/wind/CHP hybrid energy system," *Journal of Renewable and Sustainable Energy*, vol. 10, p. 045502, 2018.
- [3] J. Jannati and D. Nazarpour, "Multi-objective scheduling of electric vehicles intelligent parking lot in the presence of hydrogen storage system under peak load management," *Energy*, 2018.
- [4] P. Akbary, M. Ghiasi, M. R. R. Pourkheranjani, H. Alipour, and N. Ghadimi, "Extracting appropriate nodal marginal prices for all types of committed reserve," *Computational Economics*, pp. 1-26, 2017.
- [5] M. Ghiasi, E. Ahmadiania, M. Lariche, H. Zarrabi, and R. Simoes, "A New Spinning Reserve Requirement Prediction with Hybrid Model," *Smart Science*, vol. 6, pp. 212-221, 2018.
- [6] M. Ghiasi, M. Irani Jam, M. Teimourian, H. Zarrabi, and N. Yousefi, "A new prediction model of electricity load based on hybrid forecast engine," *International Journal of Ambient Energy*, pp. 1-8, 2017.
- [7] N. Ghadimi, A. Akbarimajd, H. Shayeghi, and O. Abedinia, "Two stage forecast engine with feature selection technique and improved meta-heuristic algorithm for electricity load forecasting," *Energy*, vol. 161, pp. 130-142, 2018/10/15/ 2018.
- [8] S. H. A. Kaboli, J. Selvaraj, and N. Rahim, "Long-term electric energy consumption forecasting via artificial cooperative search algorithm," *Energy*, vol. 115, pp. 857-871, 2016.
- [9] S. H. A. Kaboli, A. Fallahpour, J. Selvaraj, and N. Rahim, "Long-term electrical energy consumption formulating and forecasting via optimized gene expression programming," *Energy*, vol. 126, pp. 144-164, 2017.
- [10] (2018). *REN21. 2017. Renewables 2017 Global Status Report. GSR2017 Data Pack*. Available: <http://www.ren21.net/now-available-gsr2017-data-pack/>
- [11] G. F. Reed, B. M. Grainger, A. R. Sparacino, and Z.-H. Mao, "Ship to grid: Medium-voltage DC concepts in theory and practice," *IEEE Power and Energy Magazine*, vol. 10, pp. 70-79, 2012.
- [12] P. Rodriguez and K. Rouzbehi, "Multi-terminal DC grids: challenges and prospects," *Journal of Modern Power Systems and Clean Energy*, vol. 5, pp. 515-523, 2017.
- [13] J. S. Kumar, S. C. Raja, J. J. D. Nesamalar, and P. Venkatesh, "Optimizing renewable based generations in AC/DC microgrid system using hybrid Nelder-Mead-Cuckoo Search algorithm," *Energy*, vol. 158, pp. 204-215, 2018.

- [14] M. Ghiasi, "A Detailed Study for Load Flow Analysis in Distributed Power System," *International Journal of Industrial Electronics, Control and Optimization*, vol. 1, pp. 159-160, 2018.
- [15] K. Rouzbehi, J. I. Candela, G. B. Gharehpetian, L. Harnefors, A. Luna, and P. Rodriguez, "Multiterminal DC grids: Operating analogies to AC power systems," *Renewable and Sustainable Energy Reviews*, vol. 70, pp. 886-895, 2017/04/01/ 2017.
- [16] K. Rouzbehi, S. S. H. Yazdi, and N. Shariati, "Power Flow Control in Multi-Terminal HVDC Grids using a Serial-Parallel DC Power Flow Controller," *IEEE Access*, 2018.
- [17] M. B. Shadmand and R. S. Balog, "Multi-objective optimization and design of photovoltaic-wind hybrid system for community smart DC microgrid," *IEEE Transactions on Smart Grid*, vol. 5, pp. 2635-2643, 2014.
- [18] R. Chedid, H. Akiki, and S. Rahman, "A decision support technique for the design of hybrid solar-wind power systems," *IEEE transactions on Energy conversion*, vol. 13, pp. 76-83, 1998.
- [19] M. Ghiasi and J. Olamaei, "Optimal capacitor placement to minimizing cost and power loss in Tehran metro power distribution system using ETAP (A case study)," *Complexity*, vol. 21, pp. 483-493, 2016.
- [20] M. Ghiasi, N. Ghadimi, and E. Ahmadiania, "An analytical methodology for reliability assessment and failure analysis in distributed power system," *SN Applied Sciences*, vol. 1, 2019.
- [21] O. C. Onar, M. Uzunoglu, and M. S. Alam, "Modeling, control and simulation of an autonomous wind turbine/photovoltaic/fuel cell/ultra-capacitor hybrid power system," *Journal of Power Sources*, vol. 185, pp. 1273-1283, 2008/12/01/ 2008.
- [22] I. Tank and S. Mali, "Renewable based dc microgrid with energy management system," in *Signal Processing, Informatics, Communication and Energy Systems (SPICES), 2015 IEEE International Conference on*, 2015, pp. 1-5.
- [23] J. Cao and A. Emadi, "A new battery/ultracapacitor hybrid energy storage system for electric, hybrid, and plug-in hybrid electric vehicles," *IEEE Transactions on power electronics*, vol. 27, pp. 122-132, 2012.
- [24] A. Nouri, H. Khodaei, A. Darvishan, S. Sharifian, and N. Ghadimi, "Optimal performance of fuel cell-CHP-battery based micro-grid under real-time energy management: An epsilon constraint method and fuzzy satisfying approach," *Energy*, vol. 159, pp. 121-133, 2018/09/15/ 2018.
- [25] E. Kabalcı, "An islanded hybrid microgrid design with decentralized DC and AC subgrid controllers," *Energy*, vol. 153, pp. 185-199, 2018.
- [26] S. S. Sebtahmadi, H. B. Azad, S. H. A. Kaboli, M. D. Islam, and S. Mekhilef, "A PSO-DQ current control scheme for performance enhancement of Z-source matrix converter to drive IM Fed by abnormal voltage," *IEEE Transactions on Power Electronics*, vol. 33, pp. 1666-1681, 2018.
- [27] D. Kumar, F. Zare, and A. Ghosh, "DC microgrid technology: system architectures, AC grid interfaces, grounding schemes, power quality, communication networks, applications and standardizations aspects," *Ieee Access*, vol. 5, pp. 12230-12256, 2017.
- [28] Y. Sun, J. Xu, G. Lin, F. Ni, and R. Simoes, "An optimal performance based new multi-objective model for heat and power hub in large scale users," *Energy*, vol. 161, pp. 1234-1249, 2018/10/15/ 2018.

- [29] S. Jain, M. B. Shadmand, and R. S. Balog, "Decoupled Active and Reactive Power Predictive Control for PV Applications using a Grid-tied Quasi-Z-Source Inverter," *IEEE Journal of Emerging and Selected Topics in Power Electronics*, 2018.
- [30] B. Wunder, L. Ott, J. Kaiser, Y. Han, F. Fersterra, and M. März, "Overview of different topologies and control strategies for DC micro grids," in *DC Microgrids (ICDCM), 2015 IEEE First International Conference on*, 2015, pp. 349-354.
- [31] F. S. Gazijahani and J. Salehi, "Reliability constrained two-stage optimization of multiple renewable-based microgrids incorporating critical energy peak pricing demand response program using robust optimization approach," *Energy*, vol. 161, pp. 999-1015, 2018/10/15/2018.
- [32] C. A. C. Coello, G. T. Pulido, and M. S. Lechuga, "Handling multiple objectives with particle swarm optimization," *IEEE Transactions on evolutionary computation*, vol. 8, pp. 256-279, 2004.
- [33] A. Rafieerad, A. Bushroa, B. Nasiri-Tabrizi, S. Kaboli, S. Khanahmadi, A. Amiri, *et al.*, "Toward improved mechanical, tribological, corrosion and in-vitro bioactivity properties of mixed oxide nanotubes on Ti-6Al-7Nb implant using multi-objective PSO," *Journal of the mechanical behavior of biomedical materials*, vol. 69, pp. 1-18, 2017.
- [34] A. O. Haruni, M. Negnevitsky, M. E. Haque, and A. Gargoom, "A novel operation and control strategy for a standalone hybrid renewable power system," *IEEE transactions on sustainable energy*, vol. 4, pp. 402-413, 2013.
- [35] C. Bhende, S. Mishra, and S. G. Malla, "Permanent magnet synchronous generator-based standalone wind energy supply system," *IEEE Transactions on Sustainable Energy*, vol. 2, pp. 361-373, 2011.
- [36] M. Modiri-Delshad, S. H. A. Kaboli, E. Taslimi-Renani, and N. A. Rahim, "Backtracking search algorithm for solving economic dispatch problems with valve-point effects and multiple fuel options," *Energy*, vol. 116, pp. 637-649, 2016.
- [37] M. B. Shadmand, S. Jain, and R. S. Balog, "Auto-Tuning Technique for the Cost Function Weight Factors in Model Predictive Control for Power Electronics Interfaces," *IEEE Journal of Emerging and Selected Topics in Power Electronics*, 2018.
- [38] G. Aghajani and N. Ghadimi, "Multi-objective energy management in a micro-grid," *Energy Reports*, vol. 4, pp. 218-225, 2018/11/01/2018.
- [39] K. Deb, A. Pratap, S. Agarwal, and T. Meyarivan, "A fast and elitist multiobjective genetic algorithm: NSGA-II," *IEEE transactions on evolutionary computation*, vol. 6, pp. 182-197, 2002.
- [40] C. M. Fonseca and P. J. Fleming, "Genetic Algorithms for Multiobjective Optimization: Formulation Discussion and Generalization," in *Icga*, 1993, pp. 416-423.

**Highlights**

- A comprehensive analysis on new structures of AC and DC systems is provided
- An intelligent method based on multi-objective particle swarm optimization is used
- To increase the availability and reduce network costs, the capacity of a smart microgrid with hybrid RESs is determined
- Optimal design of an AC-DC hybrid microgrid is presented